

## Fluorescence Enhancement of a Single Germanium Vacancy Center in a Nanodiamond by a Plasmonic Bragg Cavity

Shailesh Kumar,<sup>1, a)</sup> Cuo Wu,<sup>1,2</sup> Danylo Komisar,<sup>1</sup> Yinhui Kan,<sup>1,3</sup> Liudmilla F. Kulikova,<sup>4</sup> Valery A. Davydov,<sup>4</sup> Viatcheslav N. Agafonov,<sup>5</sup> and Sergey I. Bozhevolnyi<sup>1,6</sup>

<sup>1)</sup>*Centre for Nano Optics, University of Southern Denmark, Campusvej 55, Odense M, DK-5230, Denmark*

<sup>2)</sup>*Institute of Fundamental and Frontier Sciences, University of Electronic Science and Technology of China, Chengdu, 610054 P. R. China*

<sup>3)</sup>*Institute of Engineering Thermophysics, Shanghai Jiao Tong University, Shanghai, 200240, China*

<sup>4)</sup>*L.F. Vereshchagin Institute for High Pressure Physics, Russian Academy of Sciences, Troitsk, Moscow, 142190, Russia*

<sup>5)</sup>*GREMAN, UMR CNRS CEA 7347, University of Tours, 37200 Tours, France*

<sup>6)</sup>*Danish Institute for Advanced Study, University of Southern Denmark, Campusvej 55, DK-5230 Odense M, Denmark*

(Dated: 15 December 2020)

This is the author's peer reviewed, accepted manuscript. However, the online version of record will be different from this version once it has been copyedited and typeset.  
PLEASE CITE THIS ARTICLE AS DOI:10.1063/1.50033507

Germanium vacancy (GeV) centers in diamonds constitute a promising platform for single-photon sources to be used in quantum information technologies. Emission from these color centers can be enhanced by utilizing a cavity that is resonant at the peak emission wavelength. We investigate circular plasmonic Bragg cavities for enhancing the emission from single GeV centers in nanodiamonds (NDs) at the zero phonon line. Following simulations of the enhancement for different configuration parameters, the appropriately designed Bragg cavities together with out-coupling gratings composed of hydrogen silsesquioxane ridges are fabricated around the NDs containing nitrogen vacancy (NV) centers deposited on a silica-coated silver surface. We characterize the fabricated configurations and finely tune the cavity parameters to match the GeV emission. Finally, we fabricate the cavity containing a single GeV-ND and compare the total decay-rate before and after the cavity fabrication, finding a decay-rate enhancement of  $\sim 5.5$  and thereby experimentally confirming the feasibility of emission enhancement with circular plasmonic cavities.

---

<sup>a)</sup>Electronic mail: shku@mci.sdu.dk

## I. INTRODUCTION

Single photon sources are an important resource for photon-based quantum technologies<sup>1-3</sup>. Different single photon sources are explored for their potential of use in quantum technologies<sup>4-7</sup>. Color centers in diamonds are one of the most promising candidates for quantum technologies. In particular, group IV defect centers have narrow emission lines with high emission in their zero phonon lines (ZPLs)<sup>8</sup>. Germanium vacancy (GeV) centers in diamonds can generate single photons at room temperature<sup>9</sup>. They have also been shown to generate single photons in lifetime-limited bandwidths, and have been utilized for integration in hybrid photonic circuits<sup>10,11</sup>. Even at room temperature, the emission peak is narrow (width less than 10nm) with 70% of emission into it. Most of the defect centers in diamonds have a lifetime in the range of 1-10ns, and they emit in all directions. This is a challenge for its use, and to enhance the decay-rate of quantum emitters and direct its emission in a single optical mode by engineering its environment has been an area of research for the last couple of decades. There are two categories of materials that are employed for engineering the environment of the emitter - dielectric and metallic<sup>12</sup>. Dielectric structures utilized for enhancement of fluorescence emission is mainly cavity structures as the cavity structure enhances the emission by increasing the interaction of the optical mode to the emitter multiple times. Therefore, with a high Q-factor of the cavity, the enhancement can be high. The high Q-factor of the cavity also results in a narrow resonance spectrum of the cavity. At room temperature, the emission spectrum of any solid-state emitter is, in general, broad. Only a part of the emission spectrum of a broadband solid-state emitter can be enhanced by fabricating a high Q dielectric cavity around the emitter<sup>13-15</sup>. Therefore, the total decay-rate is not much enhanced.

Metallic structures, on the other hand, can be utilized for the enhancement of broadband emission from solid-state single emitters. This is possible as the metallic structures can support confined modes beyond the diffraction limit, both in the form of plasmonic waveguides as well as structures supporting localized plasmonic modes. Various waveguide structures and structures supporting localized plasmonic modes have been utilized for enhancement of solid-state emitters<sup>16-35</sup>. Moreover, plasmonic metasurfaces have been utilized for obtaining polarized single photons<sup>36</sup>. Plasmonic Bragg cavities have been used for obtaining enhanced emission at zero phonon lines of NV centers<sup>37,38</sup>. Here, we utilize a circular plasmonic Bragg cavity to obtain fluorescence enhancement at ZPL of a single GeV center, and also obtain total decay-rate enhancement

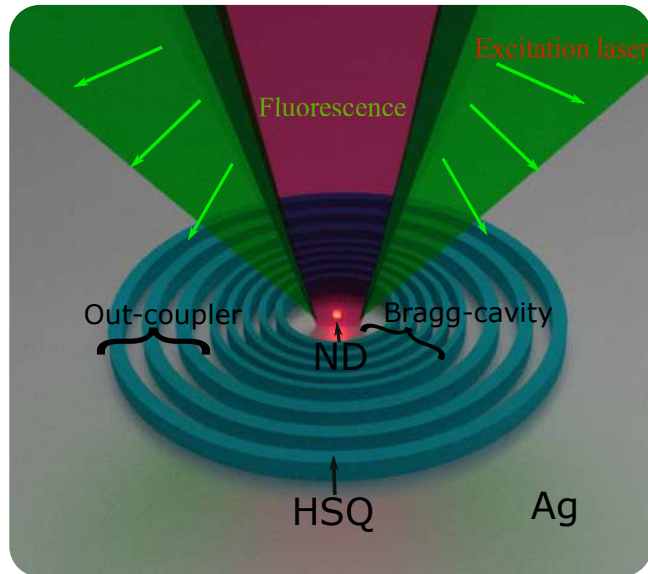


FIG. 1. A schematic of the experiment.

by up to a factor of  $\sim 5.5$ . This is possible due to the narrow emission spectrum together with relatively low  $Q$  of our plasmonic Bragg cavity.

In Figure 1, we present a schematic of the experiment. A nanodiamond (ND) containing a single GeV center is excited by a radially polarized green laser. This efficiently excites the transition dipole perpendicular to the silver surface. Dipole emitter perpendicular to silver surface excites plasmons efficiently and couples well to the plasmonic Bragg cavity, and therefore the fluorescence of the emitter is enhanced. The enhanced emission coupled to the cavity is harnessed by an out-coupler fabricated around the Bragg cavity to collect the fluorescence that is transmitted out of the cavity.

## II. SIMULATION AND EXPERIMENT

To know the expected decay-rate enhancement as well as to find the parameters of the Bragg cavity, we perform numerical simulations. The simulations are done using the finite element method (FEM) in a commercial software (COMSOL Multiphysics). Figure 2(a) and (b) show the structure that we simulate. As in experiments, we use an optically thick silver layer in simulations. A 3 nm thin Ti layer and 20nm layer of silica are used on top of the silver. GeV center is modeled as a dipole perpendicular to silver surface, emitting at a wavelength of 602nm. Refractive indices of 1.41 for hydrogen silsesquioxane (HSQ), and 1.5 for  $SiO_2$  were used. Silver and titanium

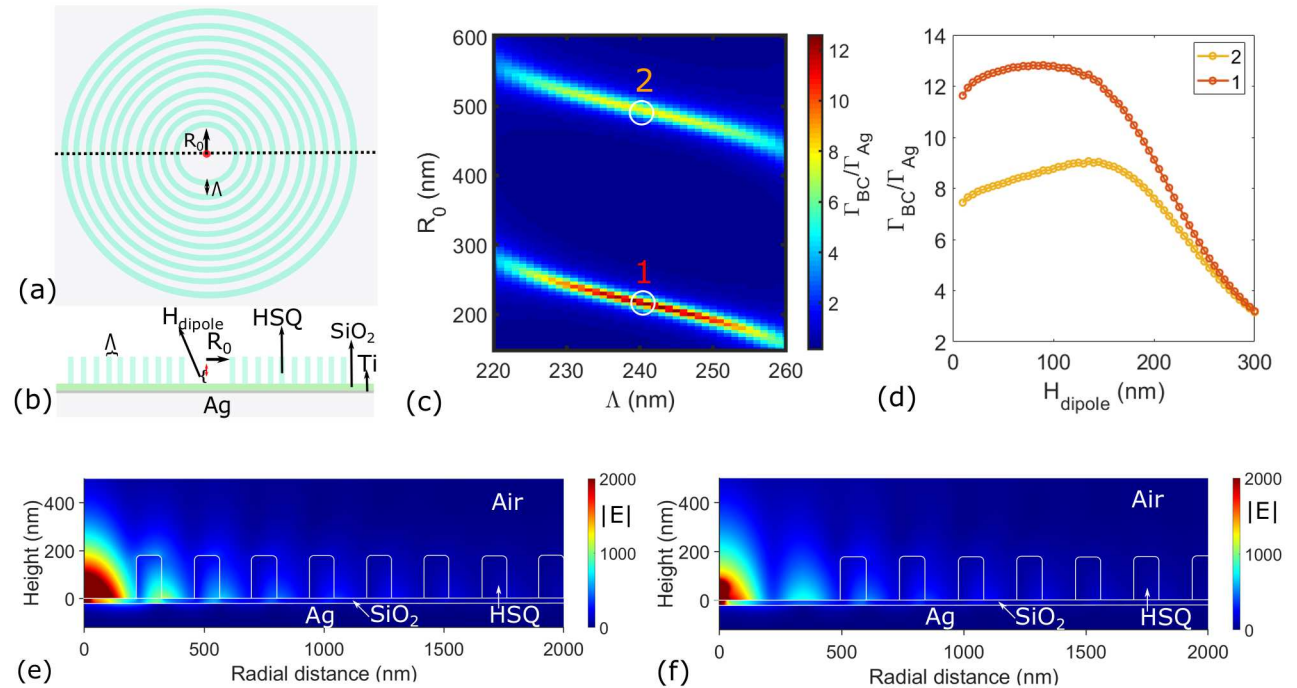


FIG. 2. (a) Top-view of the simulated structure.  $R_0$ : inner radius of Bragg cavity.  $\Lambda$ : period of Bragg cavity. (b) Cross-section along the dashed line in (a).  $H_{dipole}$ : Dipole height,  $SiO_2$ : silica, Ti: titanium, HSQ: hydrogen silsesquioxane, Ag: silver, Si: silicon. (c) Decay-rate enhancement due to the Bragg cavity normalized to decay-rate without cavity for  $H_{dipole} = 30$  nm. Numbers 1 and 2 denote the positions of fundamental and second order resonance of the cavity for a wavelength of 602 nm. (d) Decay-rate enhancement due to the Bragg cavity normalized to decay-rate without cavity as a function of  $H_{dipole}$  for the fundamental and second order resonances of the cavity, indicated in (c). (e) and (f) Electric field distributions as the Bragg cavity is excited by an electric dipole, for (e) fundamental mode and (f) second order mode.

refractive indices were used from references<sup>39,40</sup>. We vary  $R_0$ ,  $\Lambda$  and  $H_{dipole}$ , while having fixed duty cycle, ratio of HSQ ridge width to  $\Lambda$ , of  $\chi = 0.44$  to find the optimal parameters for decay-rate enhancement. In Figure 2(c), we present the decay-rate enhancement due to the Bragg cavity normalized by the decay-rate of the emitter without the cavity, at the same position ( $H_{dipole} = 30$  nm) on the surface. In the figure, two regions of high decay-rate enhancement can be seen. The first region  $R_0 < 300$  nm corresponds to the fundamental mode of the cavity. This cavity resonance corresponds to the maximum possible decay-rate enhancement. The second region  $R_0 > 300$  nm, in the Figure 2(c), corresponds to second order resonance of the cavity. The expected decay-rate enhancement is lower for the second order cavity resonance mainly due to increased cavity

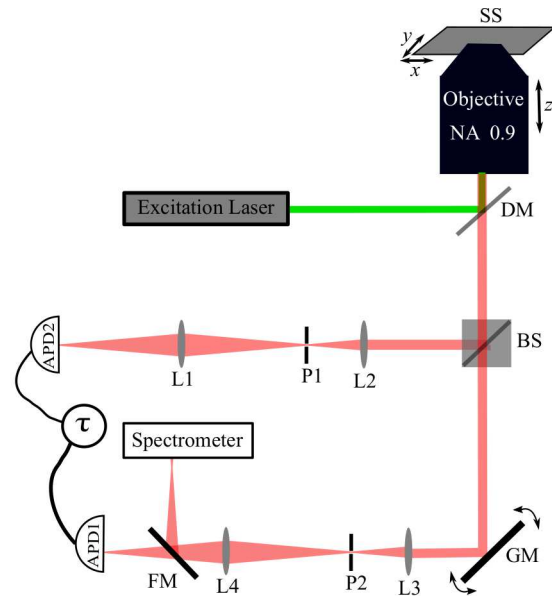


FIG. 3. A schematic of optical set-up. SS: sample stage, DM:dichroic mirror, BS: beam splitter, FM: flip mirror, L1,L2,L3,L4: lenses, P1,P2: pin-holes, GM: galvanometric mirrors, APD1,APD2: avalanche photo-diodes

volume. It should be noted that the decrease in the decay-rate enhancement is not proportional to the corresponding increase in  $R_0$  as the mode leaks into the Bragg reflector. This leakage is stronger for the fundamental than second-order resonance mode as seen in the corresponding electric field distributions [cf., Figure 2(e) and (f)]. It should also be noted that if the emitter is placed within 50nm of the center of the cavity, the decay-rate enhancement should not change significantly according to our simulations. The decay-rate enhancement is also expected to change with the change in  $H_{dipole}$ . Therefore, for the fundamental and second order cavity resonances, in Figure 2(d), we present the decay-rate enhancement as a function of  $H_{dipole}$  for fixed  $R_0$  and  $\Lambda$ . For both the cavities, when we get far from the surface ( $H_{dipole} > 180\text{nm}$ ) the total decay-rate enhancement decreases because of the decay in the electric field of the surface plasmons. When we get closer to the metallic surface, the observed decay-rate enhancement due to the cavity also decreases. This decrease is due to the increased non-surface plasmon polariton (non-radiative decay as well as radiative) decay-rates near the surface. The cavity enhances the surface-plasmon component of the decay-rate channel, and therefore as the effect of the cavity is higher in the case of the fundamental mode, the decrease in total decay-rate enhancement closer to the surface is not as pronounced as in the case of the second order cavity mode.

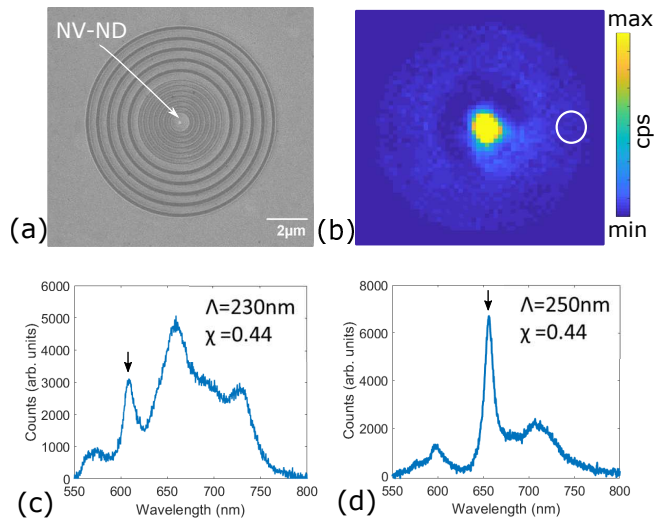


FIG. 4. (a) SEM image of a Bragg cavity out-coupler structure containing a nanodiamond with NV centers. (b) Fluorescence image obtained when the NV-ND is excited. (c) and (d) Fluorescence spectrum obtained from the region indicated in (b). Cavity parameters are included as insets, and cavity resonance wavelengths are indicated by arrows, in respective figures.

The optical set-up utilized in our work for the optical characterization of the GeV centers as well as the GeV-Bragg cavity coupled systems is schematically shown in Figure 3. We use 532nm lasers, continuous wave (CW) or pulsed with the pulse-width of 50 ps, for exciting the emitters. Same objective (numerical aperture (NA)= 0.9) is used to excite and to collect the fluorescence. The fluorescence is directed to a balanced (50/50) beam splitter. In one arm, the fluorescence is directed to an avalanche photo diode (APD2). In the other arm of the beam splitter, the fluorescence is directed to a pair of galvanometric mirrors, after which the fluorescence is passed through a pinhole, which is projected onto an APD or a spectrometer. Galvanometric mirrors help us to direct any point in the focal plane to be characterized for its spectrum, lifetimes etc. By scanning the mirrors, we also obtain an image of the focal plane while continuously illuminating the same spot. To correlate the timings of photons incident on two APDs, we utilize a PicoQuant system, and thereby measure correlation between photons detected by the APDs.

With the expected decay-rate enhancements estimated from the simulations, we now describe our experiment. In order to know the resonance wavelength of the cavity, we utilize nanodiamonds containing multiple NV centers (NV-NDs) as a fluorescence source because of their broad fluorescence spectrum. To fabricate the circular Bragg cavities with NV-NDs in their centers, we use a silicon substrate with an optically thick (200nm) thermally deposited silver (Ag) layer. A

3 nm titanium (Ti) layer and subsequently 20 nm of silica ( $SiO_2$ ) layer is deposited to protect the silver from oxidation. Gold markers are fabricated by electron-beam (e-beam) lithography on the substrates. NV-NDs are then deposited on the substrates by spin coating. After deposition of NV-NDs on the sample, a dark-field microscope image is taken. The images are then utilized with the help of gold markers to determine the location of NV-NDs on the substrate. After determining the position of NV-NDs, Bragg-cavity together with an out-coupler grating is fabricated utilizing a method that we have used before<sup>23,36</sup>. Briefly, hydrogen silsesquioxane (HSQ) solution (6% by weight) in methyl isobutyl ketone (MIBK) was spin-coated at 1200 rpm to obtain a thickness of 180nm. With e-beam, the structures consisting of Bragg-cavity and out-coupler are exposed and then developed in tetramethylammonium hydroxide (TMAH). The period for out-couplers was kept exactly two times that of the Bragg cavity. In Figure 4(a), we present a scanning electron microscope (SEM) image of a fabricated structure with NV-ND at its center indicated. Figure 4(b) shows a fluorescence image when the NV-ND at the center is excited with a 532 nm laser which is radially polarized. In addition to the direct emission from the NV-ND, we also observe emission from the out-couplers. This is the fluorescence that gets coupled to the plasmonic Bragg-cavity and is enhanced at the resonance of the cavity and part of it is coupled out of the cavity. This part is out-coupled to the far-field and is observed as radiation from the out-couplers. To determine the resonance wavelength of the cavities, we have fabricated the structures with scaled parameters and measured the spectrum observed from out-couplers. Figure 4(c) and (d) show spectra with periods ( $\Lambda$ ) of 230nm and 250nm, respectively. We have observed the cavity resonances to be at 608nm and 654 nm, respectively. By further scaling and measurement of spectra, we determined the required parameters for enhancing the decay-rate of GeV centers would be  $\Lambda$  225nm with a duty cycle of  $\chi = 0.44$ , and a value of  $R_0 = 375$ nm was used. Nanodiamonds that contain single GeV centers can vary in size from 100nm to 500nm. Therefore, we have chosen to utilize the second order resonance of the cavity instead of the fundamental resonance.

Nanodiamonds with single GeV- centers were produced by high pressure – high temperature (HPHT) synthesis based on the hydrocarbon metal catalyst-free growth system presenting homogeneous mixtures of naphthalene  $C_{10}H_8$  (Chemapol) with tetraphenylgermanium  $C_{24}H_{20}Ge$  (Sigma-Aldrich). The synthesis was performed on a high-pressure apparatus of “Toroid” type. The synthesis procedure of nanodiamonds with impurity-vacancy colour centers was similar to the one described earlier<sup>41</sup>. The chemical purification of diamond materials was carried out by processing them with a mixture of acids ( $HNO_3 - HClO_4 - H_2SO_4$ ). Aqueous dispersion of nanodiamonds

were obtained with the help of ultrasonic UP200Ht dispersant (Hielscher Ultrasonic Technology). To incorporate the GeV centers in Bragg cavities, a sample with gold markers with parameters as described above are fabricated and nanodiamonds containing GeV centers are spin-coated. The gold markers and spots in the dark-field image are utilized to locate the nanodiamonds. After determining the position of GeV containing nanodiamonds, in a  $100 \times 100 \mu\text{m}^2$  area, the spots are scanned using a 532 nm laser, and fluorescence is collected. Those nanodiamonds which are fluorescent are further characterized by measuring their spectrum, lifetime, and auto-correlation. Once enough nanodiamonds containing GeV centers are found, the Bragg-cavities together with out-couplers are fabricated following the procedure described above.

### III. RESULTS AND DISCUSSION

In Figure 5(a), spectrum of a single GeV in a nanodiamond is shown. Figure 5(b) shows the spectrum of the same GeV center after fabrication of Bragg cavity with an out-coupler. The inset shows an SEM image with a GeV-ND in the center of the structure. As can be observed, the spectrum of emitted fluorescence from the GeV center emitted directly to the far-field only slightly changes after fabrication of Bragg cavity. This is because the emission to the far-field does not interact with the cavity. In Figure 5(c), we show a fluorescence image where the GeV ND in the center is excited and fluorescence can be observed from the center as well as from the out-coupler grating, as explained in the previous section. In contrast to this similarity, the spectrum of fluorescence observed from the out-couplers shown in Figure 5(d) is markedly different: while the main peak of the spectrum clearly coincides with the peak emission of a GeV center, the phonon sideband is strongly suppressed. This shows that the fluorescence spectrum emitted into the cavity is different compared to the direct emission to the far-field. The part of emission coupled to surface plasmons is enhanced by the cavity and the spectral part enhanced can be observed from the out-couplers, as discussed in the previous section. This coupling to the Bragg cavity results in the total decay-rate enhancement as well. Now, to determine the total decay-rate enhancement due to the cavity, we compare the lifetimes measured before and after the cavity is fabricated, as measured at the GeV-ND, that is, at the center of the cavity. Figure 5(e) shows the data as well as single exponential fits ( $Ae^{-t/\tau} + \text{constant}$ ) to the lifetimes before and after fabrication. The lifetime before fabrication of the Bragg cavity was estimated to be 9.8ns, whereas the lifetime after fabrication of the nanocavity is estimated to be 1.8ns. Therefore, by comparing the lifetimes,

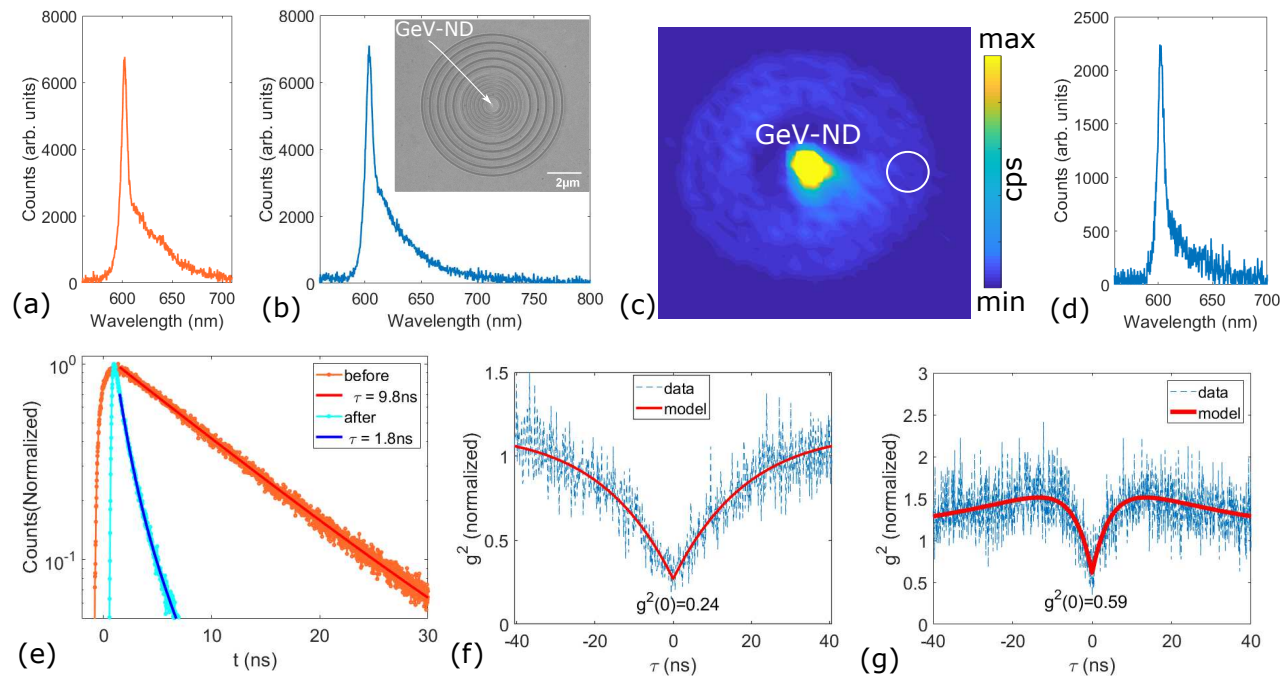


FIG. 5. (a) Spectrum of a GeV-center in a nanodiamond. (b) Spectrum of the same GeV-center in a nanodiamond after fabrication of Bragg cavity. Inset: GeV-ND in a Bragg cavity with an out-coupler. (c) Fluorescence image obtained when the GeV-ND is continuously excited with 532nm laser. (d) Fluorescence spectrum obtained from the region encircled in (c). (e) Lifetime comparison of a GeV center before and after fabrication of a Bragg cavity structure around it, measured at GeV-ND spot in (c). (f) and (g) auto-correlation of fluorescence before and after fabrication of a Bragg cavity around a GeV center, measured at GeV-ND spot in (c).

we observe a decay-rate enhancement of  $\sim 5.5$  for the GeV center. For one other such system, the decay rate enhancement was found to be  $\sim 2.6$ , as presented in Figure 6.

In simulations, for the second harmonic resonance of the cavity, we estimated an enhancement of 8. There are many reasons for the difference in the decay-rate enhancement observed in the experiment from the simulations. First, the position of the GeV center inside the nanodiamond is unknown, and depending on the position of GeV inside the nanodiamond the decay-rate enhancement will vary. Second, the inaccuracy in placing the nanodiamond in the center of the cavity which is estimated to be  $\sim 30 \text{ nm}^{25}$ . This inaccuracy alone does not account for the difference as discussed above in relation with the results shown in Figure 2. Third, the orientation of the GeV dipole may not be exactly perpendicular to the silver surface as has been assumed in the simulations, a deviation that strongly influences the plasmon excitation and thereby the total decay-rate

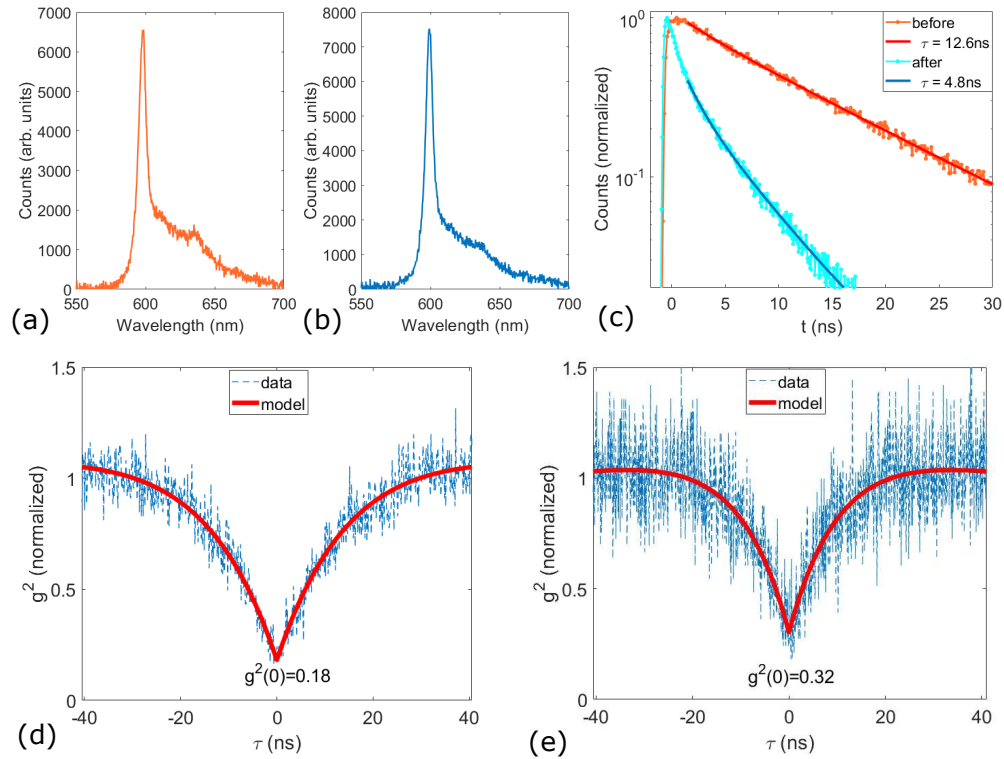


FIG. 6. (a) Spectrum of a GeV-center in a nanodiamond. (b) Spectrum of the same GeV-center in (a) after fabrication of the Bragg cavity around the nanodiamond. (c) Lifetime comparison of the GeV center before and after fabrication of the Bragg cavity. (d) and (e) auto-correlation of fluorescence before and after, respectively, fabrication of a Bragg cavity around the GeV center.

enhancement. Fourth, in the simulations a single wavelength of 602nm was used. Because of the width of the resonance ( $\sim 10$ nm), not all the wavelengths in the resonance is enhanced to the same extent, and therefore the experimentally observed decay-rate enhancement is lower. Fifth, in the experiments, we have also observed that the structure had to be scaled down in order to match the cavity resonance to the GeV center peak emission. This essentially means that the refractive indices utilized in the simulation might be slightly different for the materials that we use in the experiment. Sixth, there might be some roughness on the surfaces in the experiments that will lower down the finesse of the resonance and is not included in the simulations. Seventh, even with the protection layer, silver can get oxidized to some extent and will shift the resonance as well as decrease the finesse of the cavity, and hence will result in lower decay-rate enhancement.

To show that we have utilized a single GeV center in the cavity, we measure the auto-correlation of the fluorescence before and after the fabrication of the cavity. We have used Hanbury Brown

and Twiss set-up for measuring the auto-correlation. In Figure 5(e) and (f), we present the auto-correlation data measured as well as a model fit for the GeV center before and after the fabrication of the cavity, respectively. We observe that the  $g^2(0)$  was well below 0.5 before the cavity was fabricated, which clearly suggests that a single GeV center was incorporated in the cavity. However, after the fabrication of the cavity,  $g^2(0)$  increased to 0.59. This, we think, is due to the increase in the background fluorescence. Background fluorescence might have increased due to trace amounts of HSQ left at the site of the GeV-ND or it can happen due to oxidation of silver. For the other coupled system, presented in Figure 6, we observed  $g^2(0)$  of 0.18 and 0.32 before and after, respectively, fabrication of the Bragg cavity.

#### IV. CONCLUSION

We have investigated circular plasmonic Bragg cavities for enhancing the emission from single GeV centers in NDs at the zero phonon line. Parameters to match the cavity resonance with the ZPL of the GeV centers were found with simulations, followed by carefully fine-tuning the parameters with measured spectra from fabricated cavities containing NV-NDs. We have fabricated Bragg cavities together with out-couplers around pre-characterized nanodiamonds that contain GeV centers. By comparing the decay-rates before and after the fabrication of the Bragg cavity, we find a decay-rate enhancement of up to  $\sim 5.5$ . Here, we have used GeV centers in nanodiamonds, but other group IV color centers in diamonds have similarly narrow emission at room temperature and thus such plasmonic Bragg cavities can be used to enhance their total-decay rate as well. Furthermore, this kind of Bragg cavity can be utilized together with other meta-surface structures to obtain enhanced emission as well as the desired polarization state from a single photon solid-state emitter.

#### AUTHOR CONTRIBUTIONS

SK and CW contributed equally.

#### DATA AVAILABILITY STATEMENT

The data that support the findings of this study are available from the corresponding author upon reasonable request.

## ACKNOWLEDGMENTS

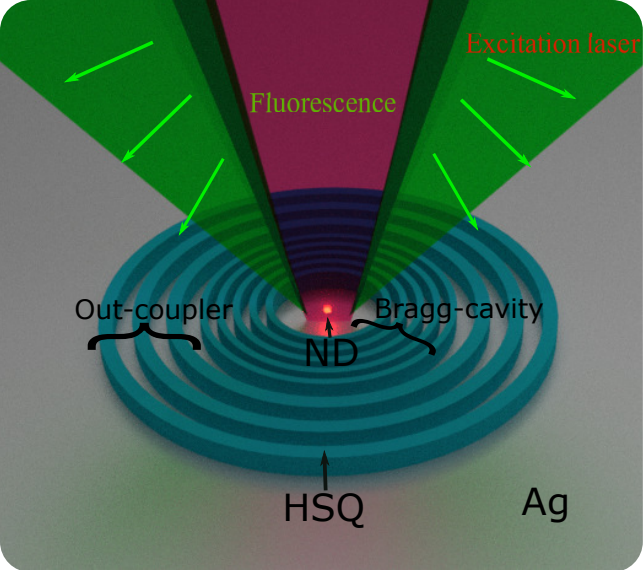
S.K. acknowledges the financial support from Villum Experiment (Grant No. 00022988). S.I.B. acknowledges the support from the Villum Kann Rasmussen Foundation (Award in Technical and Natural Sciences 2019). L.F.K. and V.A.D. thank the Russian Foundation for Basic Research for financial support (Grant 18-03-00936).

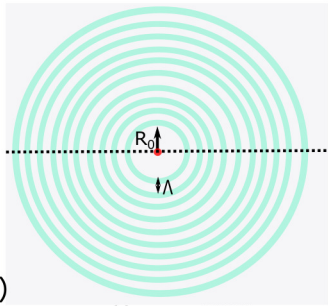
## REFERENCES

- <sup>1</sup>J. L. O'Brien, *Science* **318**, 1567 (2007).
- <sup>2</sup>J. L. O'Brien, A. Furusawa, and J. Vuckovic, *Nature Photonics* **3**, 687 (2009).
- <sup>3</sup>J. Wang, F. Sciarrino, A. Laing, and M. G. Thompson, *Nature Photonics* **14**, 273 (2020).
- <sup>4</sup>I. Aharonovich, D. Englund, and M. Toth, *Nature Photonics* **10**, 631 (2016).
- <sup>5</sup>J. D. Caldwell, I. Aharonovich, G. Cassabois, J. H. Edgar, B. Gil, and D. N. Basov, *Nature Reviews Materials* **4**, 552 (2019).
- <sup>6</sup>X. Cao, M. Zopf, and F. Ding, *Journal of Semiconductors* **40**, 7 (2019).
- <sup>7</sup>A. I. Fernández-Domínguez, S. I. Bozhevolnyi, and N. A. Mortensen, *ACS Photonics* **5**, 3447 (2018).
- <sup>8</sup>C. Bradac, W. Gao, J. Forneris, M. E. Trusheim, and I. Aharonovich, *Nature Communications* **11**, 5625 (2020).
- <sup>9</sup>T. Iwasaki, F. Ishibashi, Y. Miyamoto, Y. Doi, S. Kobayashi, T. Miyazaki, K. Tahara, K. D. Jahnke, L. J. Rogers, B. Naydenov, F. Jelezko, S. Yamasaki, S. Nagamachi, T. Inubushi, N. Mizuochi, and M. Hatano, *Scientific Reports* **5** (2015).
- <sup>10</sup>M. K. Bhaskar, D. D. Sukachev, A. Sipahigil, R. E. Evans, M. J. Burek, C. T. Nguyen, L. J. Rogers, P. Siyushev, M. H. Metsch, H. Park, F. Jelezko, M. Lončar, and M. D. Lukin, *Phys. Rev. Lett.* **118**, 223603 (2017).
- <sup>11</sup>N. H. Wan, T.-J. Lu, K. C. Chen, M. P. Walsh, M. E. Trusheim, L. De Santis, E. A. Bersin, I. B. Harris, S. L. Mouradian, I. R. Christen, E. S. Bielejec, and D. Englund, *Nature* **583** (2020).
- <sup>12</sup>S. I. Bozhevolnyi and J. B. Khurgin, *Optica* **3**, 1418 (2016).
- <sup>13</sup>A. Faraon, P. E. Barclay, C. Santori, K.-M. C. Fu, and R. G. Beausoleil, *Nature Photonics* **5**, 301 (2011).

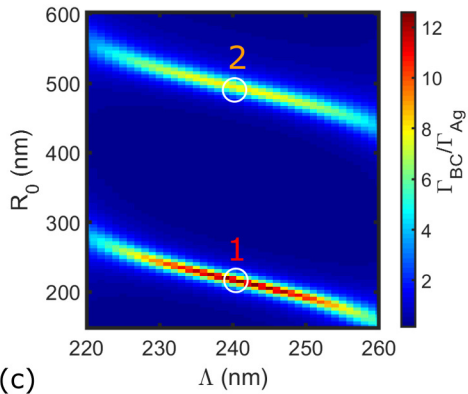
- <sup>14</sup>A. Faraon, C. Santori, Z. Huang, V. M. Acosta, and R. G. Beausoleil, *Phys. Rev. Lett.* **109**, 033604 (2012).
- <sup>15</sup>R. Høy Jensen, E. Janitz, Y. Fontana, Y. He, O. Gobron, I. P. Radko, M. Bhaskar, R. Evans, C. D. Rodríguez Rosenblueth, L. Childress, A. Huck, and U. Lund Andersen, *Phys. Rev. Applied* **13**, 064016 (2020).
- <sup>16</sup>A. V. Akimov, A. Mukherjee, C. L. Yu, D. E. Chang, A. S. Zibrov, P. R. Hemmer, H. Park, and M. D. Lukin, *Nature* **450**, 402 (2007).
- <sup>17</sup>R. Kolesov, B. Grotz, G. Balasubramanian, R. J. Stöhr, A. A. L. Nicolet, P. R. Hemmer, F. Jelezko, and J. Wrachtrup, *Nature Physics* **5**, 470 (2009).
- <sup>18</sup>A. Huck, S. Kumar, A. Shakoor, and U. L. Andersen, *Physical Review Letters* **106**, 096801 (2011).
- <sup>19</sup>S. Kumar, A. Huck, and U. L. Andersen, *Nano Letters* **13**, 1221 (2013).
- <sup>20</sup>S. Kumar, A. Huck, Y. Chen, and U. L. Andersen, *Applied Physics Letters* **102**, 103106 (2013).
- <sup>21</sup>E. Bermúdez-Ureña, C. Gonzalez-Ballester, M. Geiselmann, R. Marty, I. P. Radko, T. Holmgaard, Y. Alaverdyan, E. Moreno, F. J. Garcia-Vidal, S. I. Bozhevolnyi, and R. Quidant, *Nature Communications* **6**, 7883 (2015).
- <sup>22</sup>S. J. P. Kress, F. V. Antolinez, P. Richner, S. V. Jayanti, D. K. Kim, F. Prins, A. Riedinger, M. P. C. Fischer, S. Meyer, K. M. McPeak, D. Poulidakos, and D. J. Norris, *Nano Letters* **15**, 6267 (2015).
- <sup>23</sup>H. Siampour, S. Kumar, and S. I. Bozhevolnyi, *ACS Photonics* **4**, 1879 (2017).
- <sup>24</sup>S. Kumar, V. A. Davydov, V. N. Agafonov, and S. I. Bozhevolnyi, *Optical Materials Express* **7**, 2586 (2017).
- <sup>25</sup>H. Siampour, S. Kumar, V. A. Davydov, L. F. Kulikova, V. N. Agafonov, and S. I. Bozhevolnyi, *Light: Science and Applications* **7**, 61 (2018).
- <sup>26</sup>S. Kumar, S. K. Andersen, and S. I. Bozhevolnyi, *ACS Photonics* **6**, 23 (2019).
- <sup>27</sup>S. Kumar and S. I. Bozhevolnyi, *ACS Photonics* **6**, 1587 (2019).
- <sup>28</sup>C. Schörner, S. Adhikari, and M. Lippitz, *Nano Letters* **19**, 3238 (2019).
- <sup>29</sup>S. Kumar, T. Leißner, S. Boroviks, S. K. H. Andersen, J. Fiutowski, H.-G. Rubahn, N. A. Mortensen, and S. I. Bozhevolnyi, *ACS Photonics* **7**, 2211 (2020).
- <sup>30</sup>A. Kinkhabwala, Z. Yu, S. Fan, Y. Avlasevich, K. Muellen, and W. E. Moerner, *Nature Photonics* **3**, 654 (2009).
- <sup>31</sup>S. Schietinger, M. Barth, T. Aichele, and O. Benson, *Nano Letters* **9**, 1694 (2009).

- <sup>32</sup>T. B. Hoang, G. M. Akselrod, and M. H. Mikkelsen, *Nano Letters* **16**, 270 (2016).
- <sup>33</sup>S. K. H. Andersen, S. Kumar, and S. I. Bozhevolnyi, *Nano Letters* **17**, 3889 (2017).
- <sup>34</sup>S. I. Bogdanov, M. Y. Shalaginov, A. S. Lagutchev, C.-C. Chiang, D. Shah, A. S. Baburin, I. A. Ryzhikov, I. A. Rodionov, A. V. Kildishev, A. Boltasseva, and V. M. Shalaev, *Nano Letters* **18**, 4837 (2018).
- <sup>35</sup>S. I. Bogdanov, O. A. Makarova, X. Xu, Z. O. Martin, A. S. Lagutchev, M. Olinde, D. Shah, S. N. Chowdhury, A. R. Gabidullin, I. A. Ryzhikov, I. A. Rodionov, A. V. Kildishev, S. I. Bozhevolnyi, A. Boltasseva, V. M. Shalaev, and J. B. Khurgin, *Optica* **7**, 463 (2020).
- <sup>36</sup>Y. Kan, S. K. H. Andersen, F. Ding, S. Kumar, C. Zhao, and S. I. Bozhevolnyi, *Advanced Materials* **32**, 1907832 (2020).
- <sup>37</sup>N. P. de Leon, B. J. Shields, C. L. Yu, D. E. Englund, A. V. Akimov, M. D. Lukin, and H. Park, *Phys. Rev. Lett.* **108**, 226803 (2012).
- <sup>38</sup>H. Siampour, S. Kumar, and S. I. Bozhevolnyi, *Nanoscale* **9**, 17902 (2017).
- <sup>39</sup>E.D.Palik, *Handbook of Optical Constants* (Academic Press, 1985).
- <sup>40</sup>W. S. M. Werner, K. Glantschnig, and C. Ambrosch-Draxl, *Journal of Physical and Chemical Reference Data* **38**, 1013 (2009).
- <sup>41</sup>V. A. Davydov, A. V. Rakhmanina, S. G. Lyapin, I. D. Ilichev, K. N. Boldyrev, A. A. Shiryaev, and V. N. Agafonov, *JETP Letters* **99**, 585 (2014).

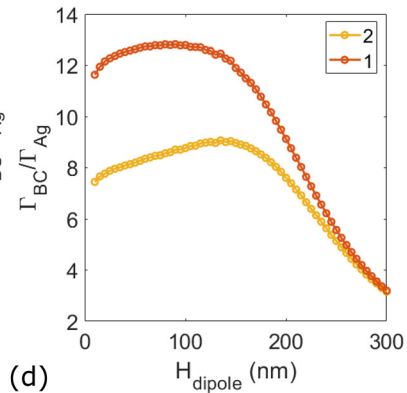




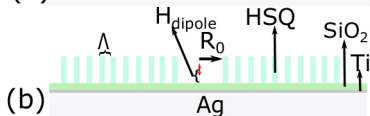
(a)



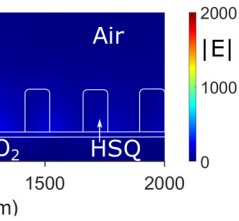
(c)



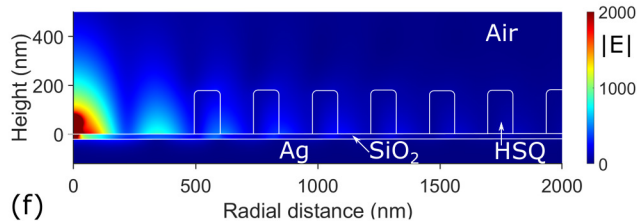
(d)



(b)



(e)



(f)

